https://doi.org/10.1130/G49141.1

Manuscript received 14 November 2020 Revised manuscript received 10 April 2021 Manuscript accepted 16 April 2021

Published online 14 June 2021

© 2021 Geological Society of America. For permission to copy, contact editing@geosociety.org

Tectonic controls on basement exhumation in the southern Rocky Mountains (United States): The power of combined zircon (U-Th)/He and K-feldspar ⁴⁰Ar/³⁹Ar thermochronology

Jason W. Ricketts¹, Jacoup Roiz¹, Karl E. Karlstrom², Matthew T. Heizler³, William R. Guenthner⁴ and J. Michael Timmons³

¹Department of Earth, Environmental and Resource Sciences, University of Texas at El Paso, El Paso, Texas 79902, USA

ABSTRACT

The Great Unconformity of the Rocky Mountain region (western North America), where Precambrian crystalline basement is nonconformably overlain by Phanerozoic strata, represents the removal of as much as 1.5 b.y. of rock record during 10-km-scale basement exhumation. We evaluate the timing of exhumation of basement rocks at five locations by combining geologic data with multiple thermochronometers. ⁴⁰Ar/³⁹Ar K-feldspar multi-diffusion domain (MDD) modeling indicates regional multi-stage basement cooling from 275 to 150 °C occurred at 1250-1100 Ma and/or 1000-700 Ma. Zircon (U-Th)/He (ZHe) dates from the Rocky Mountains range from 20 to 864 Ma, and independent forward modeling of ZHe data is also most consistent with multi-stage cooling. ZHe inverse models at five locations, combined with K-feldspar MDD and sample-specific geochronologic and/or thermochronologic constraints, document multiple pulses of basement cooling from 250 °C to surface temperatures with a major regional basement exhumation event 1300-900 Ma, limited cooling in some samples during the 770-570 Ma breakup of Rodinia and/or the 717-635 Ma snowball Earth, and ca. 300 Ma Ancestral Rocky Mountains cooling. These data argue for a tectonic control on basement exhumation leading up to formation of the Precambrian-Cambrian Great Unconformity and document the formation of composite erosional surfaces developed by faulting and differential uplift.

INTRODUCTION

The term "Great Unconformity" was first used by Dutton (1882) in Grand Canyon (Arizona, USA) and has long been recognized as a regionally important erosion surface separating Precambrian crystalline basement from overlying Phanerozoic sedimentary cover (e.g., Newberry, 1861). This contact has intrigued geologists because of the abrupt juxtaposition of igneous and metamorphic basement with the first fossiliferous Phanerozoic strata. Its regional flatness led early workers to make analogies to equally poorly understood "peneplains" (Sharp, 1940) and to articulate the erosional beveling of mountain ranges (McKee, 1969). Some workers have inferred a tectonic significance for the erosional contact, e.g., related to the supercontinent cycle (Maruyama et al., 2007; Karlstrom and

Timmons, 2012; DeLucia et al., 2017; Flowers et al., 2020) or the onset of plate tectonics (Sobolev and Brown, 2019). Other recent papers have ascribed potential global climatic/ environmental significance to this contact; e.g., as a trigger for the "Cambrian explosion" of life on Earth (Peters and Gaines, 2012) and/or deep glacial erosion associated with the Neoproterozoic snowball Earth event (Keller et al., 2019). These hypotheses are not mutually exclusive, and evaluating them requires better data on the magnitude of basement exhumation through time at regional and global scales. In the Rocky Mountains (western North America), a wide age range of sedimentary sequences (Mesoproterozoic to Jurassic) nonconformably overlie crystalline basement (Fig. 1A), which necessitates multiple great unconformities that in some

areas may have overprinted the Precambrian-Cambrian contact to create composite erosional surfaces (Karlstrom and Timmons, 2012). While the general ages of rocks above and below the various unconformities are well constrained and the thicknesses of sedimentary successions are known (Fig. 1A), the timing of basement exhumation beneath the Great Unconformity is not.

We present zircon (U-Th)/He (ZHe) and ⁴⁰Ar/³⁹Ar K-feldspar thermochronologic data from crystalline basement samples beneath the Great Unconformity at five locations in the southern Rocky Mountains of Colorado and New Mexico (Fig. 1). Our goal is to use the combined interpretive power of both thermochronologic systems to get at nuanced time-temperature (t-T) models of rocks prior to formation of the Precambrian-Cambrian Great Unconformity. K-feldspar multi-diffusion domain (MDD) modeling (275-175 °C; McDougall and Harrison, 1999) is complementary to forward and inverse modeling of ZHe data (210-50 °C; Guenthner et al., 2013; Johnson et al., 2017) in reconstructing continuous t-T models to track rock cooling to near-surface temperatures. We use an innovative approach where MDD models inform subsequent forward and inverse ZHe models (McDannell et al., 2019). Zircon grains have variable closure temperatures due to accumulation of varying degrees of radiation damage, as measured by effective uranium concentration (eU = [U] + 0.235[Th]) (Guenthner et al., 2013), and multiple singlegrain ZHe dates from the same sample show ZHe date-eU correlations that can be modeled to reconstruct possible t-T curves. Our thermal models capture multiple pulses of cooling at

²Department of Earth and Planetary Sciences, University of New Mexico, Albuquerque, New Mexico 87131, USA

³New Mexico Bureau of Geology and Mineral Resources, New Mexico Institute of Mining and Technology, Socorro, New Mexico 87801. USA

⁴Department of Geology, University of Illinois at Urbana-Champaign, Urbana, Illinois 61801, USA

CITATION: Ricketts, J.W., et al., 2021, Tectonic controls on basement exhumation in the southern Rocky Mountains (United States): The power of combined zircon (U-Th)/He and K-feldspar 40Ar/39Ar thermochronology: Geology, v. 49, p. 1187–1192, https://doi.org/10.1130/G49141.1

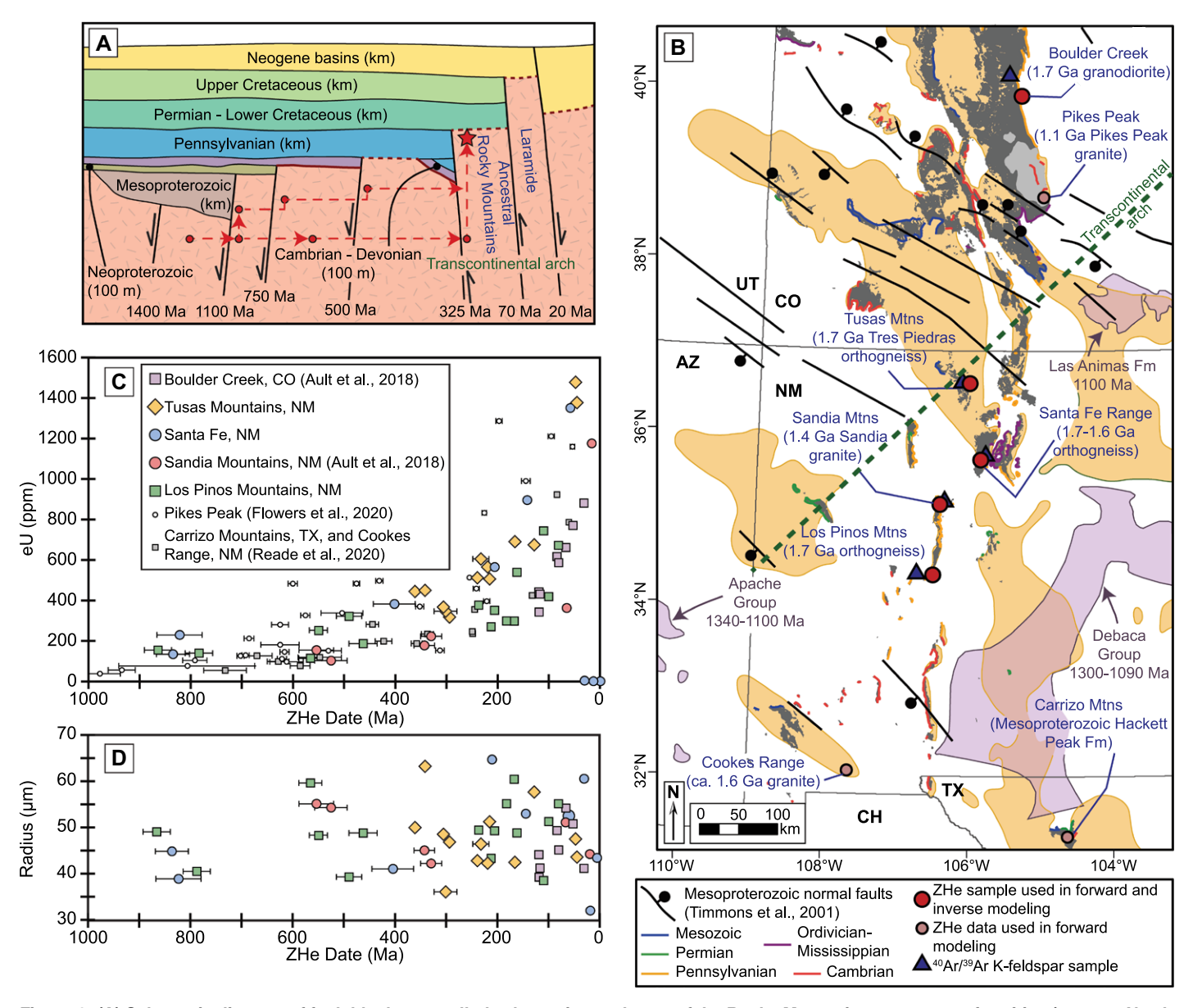


Figure 1. (A) Schematic diagram of fault block–controlled exhumation and ages of the Rocky Mountains great unconformities (western North America). Times (in Ma) and approximate scales of kilometers (km in parentheses) of relative block uplift and subsidence are shown. For samples collected below the Permian unconformity (red star), thermochronology may decipher multi-stage versus single-event cooling (red dashed lines). Dark-red contact represents the Precambrian-Cambrian Great Unconformity, and dashed dark-red lines indicate composite erosional surfaces. (B) Study area within the southern Rocky Mountains and sample locations. Dark gray polygons are Precambrian rock; light gray is the Pikes Peak batholith. Colored lines indicate exposures of the Great Unconformity, color-coded by age of overlying sediment. Orange polygons are Ancestral Rocky Mountains uplifts, and purple polygons are Proterozoic sedimentary deposits. UT—Utah; CO—Colorado; AZ—Arizona; NM—New Mexico; CH—Chihuahua, Mexico; TX—Texas; Mtns—Mountains; Fm.—Formation. (C) Zircon (U-Th)/He (ZHe) date versus effective uranium concentration (eU) plot for locations in B. Error bars are 2σ. (D) ZHe date versus spherical grain radius.

each sample site over hundreds of millions of years, highlight the utility of combining ZHe and ⁴⁰Ar/³⁹Ar K-feldspar data to constrain upper crustal thermal histories, and indicate tectonic control in basement cooling prior to formation of the Great Unconformity as a globally significant erosional surface.

POTASSIUM FELDSPAR ⁴⁰Ar/³⁹Ar DATA AND MDD MODELING

Age spectra and t-T paths from MDD modeling of K-feldspar 40 Ar $^{/39}$ Ar data are presented from four new samples and one pre-

viously reported sample (Santa Fe Range, New Mexico; Sanders et al., 2006) (Fig. 2; see the supplemental text and Tables S1 and S2 in the Supplemental Material¹). These models reveal regional variations in the timing of cooling of

¹Supplemental Material. Detailed forward and inverse modeling methods, and Tables S1–S4 (K-feldspar sample information and analytical data, ZHe data, and complete ZHe modeling inputs, assumptions, and modeling parameters). Please visin https://doi.org/10.1130/GEOL.S.14699709 to access the supplemental material, and contact editing@geosociety.org with any questions.

Rocky Mountains basement rocks from 275 to 175 °C with important pulses at 1250–1100 Ma and 1000–700 Ma recorded in different regions. Three samples (Tusas Mountains, Santa Fe Range, and Los Pinos Mountains in New Mexico) were at >150 °C, hence at depths of >5–6 km, until after ca. 800–700 Ma.

ZIRCON (U-Th)/He DATA AND MODELING

From basement samples in the same areas as ⁴⁰Ar/³⁹Ar K-feldspar samples, a total of 37 new single-grain ZHe dates are presented from New

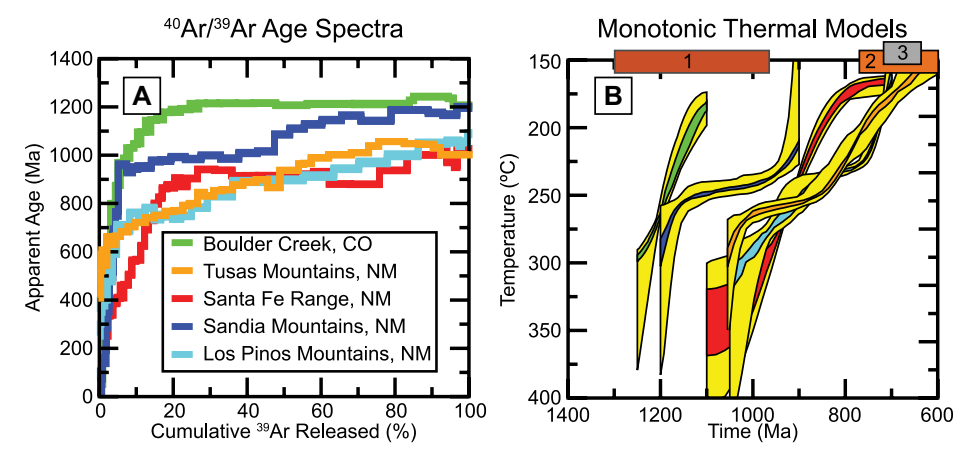


Figure 2. ⁴⁰Ar/³⁹Ar K-feldspar age spectra (A) and multi-diffusion domain time-temperature models (B) for samples plotted in Figure 1B. Yellow bands represent 90% confidence intervals of the entire distribution, and colored zones are the 90% confidence interval of the mean. Santa Fe Range sample is from Sanders et al. (2006). 1—assembly of Rodinia; 2—breakup of Rodinia; 3—snowball Earth. CO—Colorado; NM—New Mexico.

Mexico (Tusas Mountains, Santa Fe Range, and Los Pinos Mountains) (Fig. 1B). These are combined with six previously published ZHe dates from the Sandia Mountains, New Mexico, and eight ZHe dates from Boulder Creek, Colorado (Ault et al., 2018), resulting in a total of 51 ZHe dates from five samples that we used to evaluate unroofing of basement crystalline rock prior to deposition of overlying Paleozoic strata.

ZHe data from the combined samples reveal a regionally consistent ZHe date–eU envelope with large intrasample variability in ZHe dates from 20 to 864 Ma across an eU range of 100–1477 ppm (Fig. 1C; Table S3). ZHe dates from each sample show well-defined correlations with eU, with the oldest ZHe dates corresponding to low-eU grains. The data collectively define a shallow positive slope for eU values ranging from 0 to 600 ppm with an inflection to steeper

slope at higher eU. Grain size is not a dominant control on variation in ZHe dates (Fig. 1D).

Forward Modeling

Forward modeling of the composite data provides an opportunity for evaluating single-pulse Proterozoic cooling within the Rocky Mountains region versus stepwise progressive cooling (Fig. 3). For each forward model, we used an input t-T path and a mean zircon grain radius, which are used to calculate predicted ZHe dates as a function of eU (Guenthner, 2021) using helium diffusion kinetics (Guenthner et al., 2013). In Figure 3, the gray envelope for each calculation represents one standard deviation of grain size (see the Supplemental Material for complete modeling details). These plots examine a greater area than that shown in Figure 1 by also adding ZHe data from the Front Range, Colorado (Johnson et al., 2017), and the Bighorn Mountains and Wind River Range, Wyoming (Orme et al., 2016). We used a generalized thermal history of the Rocky Mountains with constraints at 350 °C at 1.4 Ga (from 40Ar/39Ar muscovite data; Shaw et al., 2005), Paleozoic cooling to surface temperatures between 550 and 310 Ma (based on ages of cover rocks), and maximum Cenozoic temperature of 125 °C at 80 Ma (from the Cretaceous sedimentary record and apatite fission-track data; e.g., Kelley and Chapin, 1995). Figure 3A tests modeled ZHe

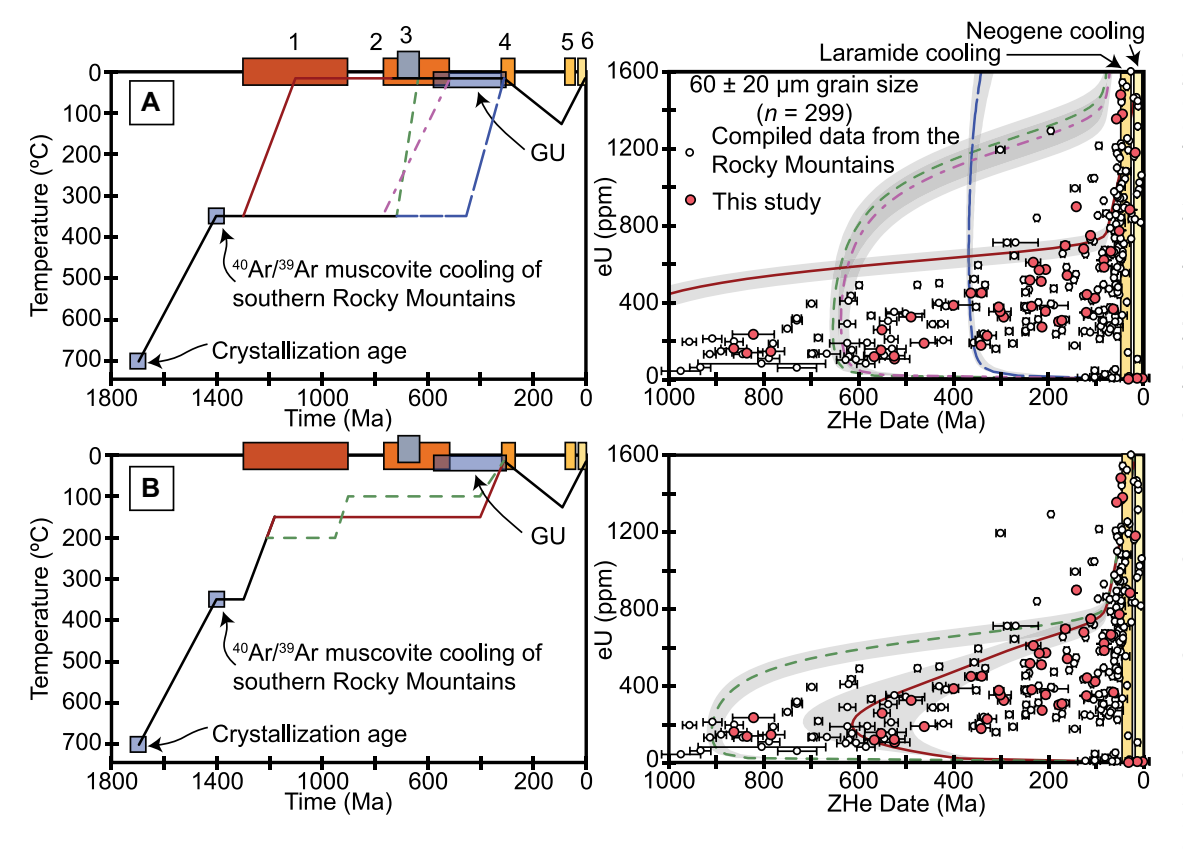


Figure 3. Forward modeling and calculated zircon (U-Th)/He (ZHe) date-effective uranium concentration (eU) trends for six Precambrian cooling paths (four paths in A, two in B). For intuitive comparison with accompanying timetemperature plots, ZHe date-eU plots show the ZHe date decreasing to the right on the x-axis and eU increasing upward on the y-axis because lowereU grains have higher closure temperatures. (A) Paths that only include single pulse of cooling. (B) Paths that include multi-stage cooling. Gray envelope represents ±1 grain size standard deviation. Error bars are 2σ. Complete data set for the entire Rocky Mountains (North America), with new and compiled ZHe data (Orme et al., 2016; Johnson et al., 2017; Ault et al., 2018; Flowers et al., 2020: Reade et al., 2020) shown (white circles) for comparison to calculated

curves. 1—assembly of Rodinia; 2—breakup of Rodinia; 3—snowball Earth; 4—Ancestral Rocky Mountains; 5—Laramide orogeny; 6—Neogene exhumation; GU—Great Unconformity.

date-eU patterns that would be generated from single-event cooling during 1300-1100 Ma assembly of Rodinia and deposition of the 1-km-

thick Debaca Group (Amarante et al., 2005); 770–570 Ma breakup of Rodinia (Yonkee et al., 2014); 717–635 Ma snowball Earth (Rooney

et al., 2014); and 350–300 Ma Ancestral Rocky Mountains orogeny (Dickinson and Lawton, 2003). Figure 3B tests multi-stage cooling

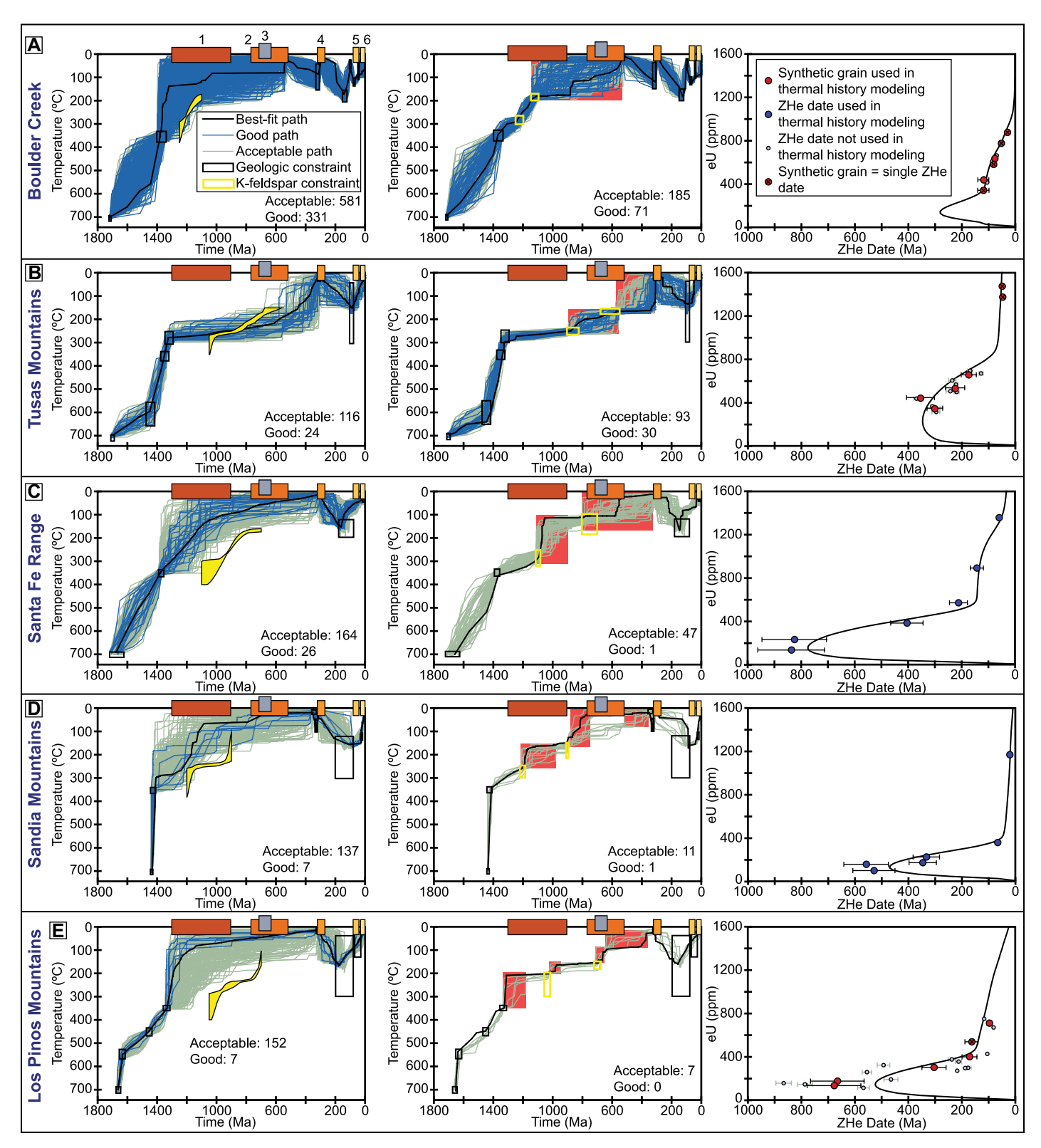


Figure 4. Inverse modeling results for five Rocky Mountains (North America) locations. Each Monte Carlo simulation tested 100,000 random paths. Yellow polygons in left panels show multi-diffusion domain models from Figure 2. Red boxes in middle panels highlight times of rapid (>10 °C/Ma) cooling in each sample. Panels on right compare input grains with calculated zircon (U-Th)/He (ZHe) date–effective uranium concentration (eU) curve modeled using best-fit path. Error bars for light and dark blue symbols are 2σ. Error bars for red symbols are 15% of the ZHe date. 1—assembly of Rodinia; 2—breakup of Rodinia; 3—snowball Earth; 4—Ancestral Rocky Mountains; 5—Laramide orogeny; 6—Neogene exhumation.

involving episodes at 1300–1200 Ma, 950–900 Ma, and 400–300 Ma. These models show different maximum preserved dates for low-eU grains, different slopes for the correlation of decreasing date with increasing eU, a slope inflection that varies from 700 to 1500 ppm eU, and a sharp near-vertical segment where similar dates for a full range of eU grains suggest rapid Cenozoic cooling. Multi-stage cooling models with a component of pre–1 Ga cooling (Fig. 3B) are most consistent with the compiled date-eU pattern than the single-stage cooling paths (Fig. 3A), as also supported by the independent K-feldspar MDD models (Fig. 2).

Inverse Modeling

Inverse modeling using HeFTy version 1.9.3 software (Ketcham, 2005) builds upon the forward-modeling results and evaluates compatibility between ZHe data and other sample-specific thermochronologic and geologic constraints. Whereas our forward models test ZHe date dispersion due to the effects of radiation damage and grain size, U and Th zonation can introduce second-order effects on resulting ZHe date-eU relationships (e.g., Hourigan et al., 2005). To account for this, we used a synthetic-grain approach similar to that of previous authors (e.g., DeLucia et al., 2018; Flowers et al., 2020; Reade et al., 2020). Synthetic grains have the mean ZHe date and eU calculated by grouping ZHe dates into eU bins. Input errors are 15% of the synthetic grain date. Table S4 includes all modeling inputs, methods, and assumptions, following methods outlined by Flowers et al. (2015). In each model, Paleozoic constraint boxes vary depending on age of overlying strata, Cenozoic constraint boxes are based on known apatite thermochronology (e.g., Ricketts et al., 2016), and all models are compatible with the minor amount of post-Cambrian argon loss observed in the K-feldspar age spectra (Sanders et al., 2006) (Figs. S1-S5).

Figure 4 (left column) shows inverse models without K-feldspar constraints but with the independently determined MDD models shown in yellow for comparison. Models agree reasonably well for the temperature range 275–175 °C, although Santa Fe Range and Sandia Mountains MDD models only narrowly overlap with higher-temperature acceptable fit paths, and the Los Pinos Mountains MDD model predicts 50 °C higher temperatures than ZHe data. This suggests an incomplete understanding of diffusion kinetics for both systems and/or potential zoning in zircon grains (e.g., Hourigan et al., 2005). Nevertheless, these relatively unconstrained ZHe models indicate variable times of cooling across the region.

The middle column in Figure 4 shows refined inverse models that incorporate additional constraint boxes (in yellow) derived from MDD models that are markedly more constrained than

those that omit K-feldspar data. These models reveal where the ZHe data provide additional constraints on times of rapid cooling (red boxes). Best-fit paths from these models have predicted ZHe date-eU curves that overlap with observed ZHe dates (Fig. 4, right column). Four of the samples are consistent with a pulse of cooling coeval with the ca. 1.0 Ga assembly of Rodinia, and Los Pinos Mountains also shows earlier ZHe-predicted cooling at 1.3-1.2 Ga. Various samples also show rapid cooling coincident with younger tectonic events such as the 770-570 Ma breakup of Rodinia and the 325 Ma Ancestral Rocky Mountains orogeny. Some samples are permissive of rapid cooling during the 717-635 Ma snowball Earth (Keller et al., 2019), although the Sandia Mountains model shows no cooling during this event. Models suggest that basement cooling to near-surface temperatures was at 520-310 Ma in the Tusas Mountains and 640-310 Ma in the Los Pinos Mountains.

DISCUSSION OF MODELING

Our study demonstrates that combining multiple thermochronometers provides a powerful empirical approach for obtaining more meaningful thermal histories. ZHe modeling is like a seesaw between early and later cooling histories such that independently constraining any part of a thermal history allows ZHe data to more tightly constrain older or younger segments. It may be intuitively surprising that 600-900 Ma ZHe dates can constrain pre-900 Ma cooling and that the overall date-eU pattern is simultaneously sensitive to post-120 °C cooling. We explore this with a series of inverse models for the Los Pinos Mountains sample (Fig. S7) that progressively add constraint boxes from other data sets to show that thermal histories become better constrained at other segments of the thermal history that are far removed from the input constraints. These help to highlight the benefit of coupling ZHe data with additional thermochronometers at both higher and lower temperatures and, in particular for this research, the added benefit of combining with K-feldspar MDD models.

PRECAMBRIAN COOLING AND FORMATION OF THE GREAT UNCONFORMITY

Forward and inverse ZHe modeling combined with 40 Ar/ 39 Ar K-feldspar modeling indicates multi-stage exhumation of Rocky Mountains basement from middle crustal depths of $\sim 10 \text{ km}$ (>275 °C) to the surface rather than a single pulse of exhumation to form the Great Unconformity. Inverse models are not consistent with the hypothesis that global Neoproterozoic glacial erosion removed 3–5 km of material during the 717–635 Ma snowball Earth (Keller et al., 2019), similar to ZHe inverse modeling

results at Pikes Peak, Colorado (Flowers et al., 2020). However, the Boulder Creek, Tusas Mountains, and Los Pinos Mountains samples permit 50-100 °C of cooling ($\sim 1-3$ km of unroofing) within a longer 800-500 Ma interval.

Our final ZHe inverse models (Fig. 4) suggest differential cooling across the region. A dominant pulse from 1300 to 1000 Ma is interpreted to reflect formation of an orogenic plateau behind the Grenville collisional boundary (Whitmeyer and Karlstrom, 2007), where differences between samples are interpreted to reflect a sample's position relative to faults in the intracratonic region >1000 km from any plate boundary (Sanders et al., 2006). Grenville-age intracratonic block faulting took place during northwest-directed contraction and northeastdirected extension and resulted in basins for Debaca Group and Las Animas Formation deposition (Marshak et al., 2000; Timmons et al., 2001). Similar cooling paths are modeled in ZHe data from the Carrizo Mountains, Texas, which lie along the Grenville continent-continent collisional front, and these samples also record a later cooling pulse from 600 to 530 Ma (Reade et al., 2020). Limited basement exhumation may have taken place in some areas in the Neoproterozoic to Cambrian, e.g., in the Tusas and Los Pinos Mountains and the midcontinent (DeLucia et al., 2017), but greater exhumation (as much as several kilometers) occurred as basement rocks in Ancestral Rocky Mountains uplifts reached the surface below Pennsylvanian-Permian strata (this study) during diachronous closure of the Ouachita suture (Dickinson and Lawton, 2003) and/or compression from the southwestern margin of Laurentia (Leary et al., 2017). The combined data document multiple pulses of fault-related exhumation prior to and after formation of the Precambrian-Cambrian Great Unconformity to form composite erosional surfaces. We propose that this tectonic paradigm for composite great unconformities may also apply to other regions (e.g., McDannell et al., 2019; Flowers et al., 2020) and continents (Guenthner et al., 2017) and that combined thermochronologic methods may help distinguish multiple basement cooling and/or unroofing episodes.

ACKNOWLEDGMENTS

Funding for this research comes from U.S. National Science Foundation grants EAR-1624538 to J.W. Ricketts and EAR-028463 and EAR-9902955 to K.E. Karlstrom and M.T. Heizler. We thank Kendra Murray, Shanan Peters, three anonymous reviewers, and Science Editor William Clyde for helpful comments that greatly improved the paper.

REFERENCES CITED

Amarante, J.F.A., Kelley, S.A., Heizler, M.T., Barnes, M.A., Miller, K.C., and Anthony, E.Y., 2005, Characterization and age of the Mesoproterozoic Debaca sequence in the Tucumcari Basin, New Mexico, *in* Karlstrom, K.E., and Keller, G.R., eds., The Rocky Mountain Region—An

- Evolving Lithosphere: Tectonics, Geochemistry, and Geophysics: American Geophysical Union Geophysical Monograph 154, p. 185–199, https://doi.org/10.1029/154GM13.
- Ault, A.K., Guenthner, W.R., Moser, A.C., Miller, G.H., and Refsnider, K.A., 2018, Zircon grain selection reveals (de)coupled metamictization, radiation damage, and He diffusivity: Chemical Geology, v. 490, p. 1–12, https://doi.org/10.1016/ j.chemgeo.2018.04.023.
- DeLucia, M.S., Guenthner, W.R., Marshak, S., Thomson, S.N., and Ault, A.K., 2018, Thermochronology links denudation of the Great Unconformity surface to the supercontinent cycle and snowball Earth: Geology, v. 46, p. 167–170, https://doi.org/10.1130/G39525.1.
- Dickinson, W.R., and Lawton, T.F., 2003, Sequential intercontinental suturing as the ultimate control for Pennsylvanian Ancestral Rocky Mountains deformation: Geology, v. 31, p. 609–612, https://doi.org/10.1130/0091-7613(2003)031<0609:SIS ATU>2.0.CO;2.
- Dutton, C.E., 1882, Tertiary history of the Grand Cañon District, with atlas: U.S. Geological Survey Monograph 2, scale, 250,000, 264 p., https://doi .org/10.3133/m2.
- Flowers, R.M., Farley, K.A., and Ketcham, R.A., 2015, A reporting protocol for thermochronologic modeling illustrated with data from Grand Canyon: Earth and Planetary Science Letters, v. 432, p. 425–435, https://doi.org/10.1016/j.epsl.2015.09.053.
- Flowers, R.M., Macdonald, F.A., Siddoway, C.S., and Havranek, R., 2020, Diachronous development of Great Unconformities before Neoproterozoic Snowball Earth: Proceedings of the National Academy of Sciences of the United States of America, v. 117, p. 10,172–10,180, https://doi.org/10.1073/pnas.1913131117.
- Guenthner, W.R., 2021, Implementation of an alpha damage annealing model for zircon (U-Th)/He thermochronology with comparison to a zircon fission track annealing model: Geochemistry Geophysics Geosystems, v. 22, e2019GC008757, https://doi.org/10.1029/2019GC008757.
- Guenthner, W.R., Reiners, P.W., Ketcham, R.A., Nasdala, L., and Giester, G., 2013, Helium diffusion in natural zircon: Radiation damage, anisotropy, and the interpretation of zircon (U-Th)/He thermochronology: American Journal of Science, v. 313, p. 145–198, https://doi.org/10.2475/03.2013.01.
- Guenthner, W.R., Reiners, P.W., Drake, H., and Tillberg, M., 2017, Zircon, titanite, and apatite (U-Th)/He ages and age-eU correlations from the Fennoscandian shield, southern Sweden: Tectonics, v. 36, p. 1254–1274, https://doi.org/10.1002/2017TC004525.
- Hourigan, J.K., Reiners, P.W., and Brandon, M.T., 2005, U-Th zonation-dependent alpha-ejection in (U-Th)/He chronometry: Geochimica et Cosmochimica Acta, v. 69, p. 3349–3365, https://doi .org/10.1016/j.gca.2005.01.024.
- Johnson, J.E., Flowers, R.M., Baird, G.B., and Mahan, K.H., 2017, "Inverted" zircon and apatite (U-Th)/He dates from the Front Range, Colorado: High-damage zircon as a low-temperature (<50 °C) thermochronometer: Earth and Planetary Science Letters, v. 466, p. 80–90, https://doi.org/10.1016/j.epsl.2017.03.002.
- Karlstrom, K.E., and Timmons, J.M., 2012, Many unconformities make one 'Great Unconformity',

- *in* Timmons, J.M., and Karlstrom, K.E., eds. Grand Canyon Geology: Two Billion Years of Earth's History: Geological Society of America Special Paper 489, p. 73–79, https://doi.org/10.1130/2012.2489(04).
- Keller, C.B., Husson, J.M., Mitchell, R.N., Bottke, W.F., Gernon, T.M., Boehnke, P., Bell, E.A., Swanson-Hysell, N.L., and Peters, S.E., 2019, Neoproterozoic glacial origin of the Great Unconformity: Proceedings of the National Academy of Sciences of the United States of America, v. 116, p. 1136–1145, https://doi.org/10.1073/ pnas.1804350116.
- Kelley, S.A., and Chapin, C.E., 1995, Apatite-fission-track thermochronology of southern Rocky Mountain–Rio Grande rift–Western High Plains Province, in Bauer, P.W., et al., eds., Geology of the Santa Fe Region: New Mexico Geological Society 46th Annual Fall Field Conference Guidebook, p. 87–96.
- Ketcham, R.A., 2005, Forward and inverse modeling of low-temperature thermochronometry data, *in* Reiners, P.W., and Ehlers, T.A., eds., Low-Temperature Thermochronology: Techniques, Interpretations, and Applications: Reviews in Mineralogy and Geochemistry, v. 58, p. 275–314, https://doi.org/10.1515/9781501509575-013.
- Leary, R.J., Umhoefer, P., Smith, M.E., and Riggs, N., 2017, A three-sided orogeny: A new tectonic model for Ancestral Rocky Mountain uplift and basin development: Geology, v. 45, p. 735–738, https://doi.org/10.1130/G39041.1.
- Marshak, S., Karlstrom, K., and Timmons, J.M., 2000, Inversion of Proterozoic extensional faults: An explanation for the pattern of Laramide and Ancestral Rockies intracratonic deformation, United States: Geology, v. 28, p. 735–738, https://doi. org/10.1130/0091-7613(2000)28<735:IOPEFA >2.0.CO:2.
- Maruyama, S., Santosh, M., and Zhao, D., 2007, Superplume, supercontinent, and post-perovskite: Mantle dynamics and anti-plate tectonics on the core-mantle boundary: Gondwana Research, v. 11, p. 7–37, https://doi.org/10.1016/j.gr.2006.06.003.
- McDannell, K.T., Schneider, D.A., Zeitler, P.K., O'Sullivan, P.B., and Issler, D.R., 2019, Reconstructing deep-time histories from integrated thermochronology: An example from southern Baffin Island, Canada: Terra Nova, v. 31, p. 189–204, https://doi.org/10.1111/ter.12386.
- McDougall, I., and Harrison, T.M., 1999, Geochronology and Thermochronology by the ⁴⁰Ar/³⁹Ar Method: Oxford, UK, Oxford University Press 269 p.
- McKee, E.D., 1969, Stratified rocks of the Grand Canyon: Chapter B *in* The Colorado River Region and John Wesley Powell: U.S. Geological Survey Professional Paper 669-B, p. 23–58, https://doi.org/10.3133/pp669B.
- Newberry, J.S., 1861, Report upon the Colorado River of the West, Part III: Geological report: Washington, D.C., U.S. Government Printing Office, 154 p.
- Orme, D.A., Guenthner, W.R., Laskowski, A.K., and Reiners, P.W., 2016, Long-term tectonothermal history of Laramide basement from zircon-He age-eU correlations: Earth and Planetary Science Letters, v. 453, p. 119–130, https://doi .org/10.1016/j.epsl.2016.07.046.
- Peters, S.E., and Gaines, R.R., 2012, Formation of the 'Great Unconformity' as a trigger for the Cambrian explosion: Nature, v. 484, p. 363–366, https://doi.org/10.1038/nature10969.

- Reade, N.Z., Biddle, J.M., Ricketts, J.W., and Amato, J.M., 2020, Zircon (U-Th)/He thermochronologic constraints on the long-term thermal evolution of southern New Mexico and western Texas: Lithosphere, v. 2020, 8881315, https://doi.org/10.2113/2020/8881315.
- Ricketts, J.W., Kelley, S.A., Karlstrom, K.E., Schmandt, B., Donahue, M.S., and van Wijk, J., 2016, Synchronous opening of the Rio Grande rift along its entire length at 25–10 Ma supported by apatite (U-Th)/He and fission-track thermochronology, and evaluation of possible driving mechanisms: Geological Society of America Bulletin, v. 128, p. 397–424, https://doi.org/10.1130/B31223.1.
- Rooney, A.D., Macdonald, F.A., Strauss, J.V., Dudás, F.Ö., Hallmann, C., and Selby, D., 2014, Re-Os geochronology and coupled Os-Sr isotope constraints on the Sturtian snowball Earth: Proceedings of the National Academy of Sciences of the United States of America, v. 111, p. 51–56, https://doi.org/10.1073/pnas.1317266110.
- Sanders, R.E., Heizler, M.T., and Goodwin, L.B., 2006, 40Ar/39Ar thermochronology constraints on the timing of Proterozoic basement exhumation and fault ancestry, southern Sangre de Cristo Range, New Mexico: Geological Society of America Bulletin, v. 118, p. 1489–1506, https:// doi.org/10.1130/B25857.1.
- Sharp, R.P., 1940, Ep-Archean and Ep-Algonkian erosion surfaces, Grand Canyon, Arizona: Geological Society of America Bulletin, v. 51, p. 1235–1269, https://doi.org/10.1130/GSAB-51-1235.
- Shaw, C.A., Heizler, M.T., and Karlstrom, K.E., 2005, 40Ar/39Ar thermochronologic record of 1.45–1.35 Ga intracontinental tectonism in the southern Rocky Mountains: Interplay of conductive and advective heating with intracontinental deformation, in Karlstrom, K.E., and Keller, G.R., eds., The Rocky Mountain Region—An Evolving Lithosphere: Tectonics, Geochemistry, and Geophysics: American Geophysical Union Geophysical Monograph 154, p. 163–184, https:// doi.org/10.1029/154GM12.
- Sobolev, S.V., and Brown, M., 2019, Surface erosion events controlled the evolution of plate tectonics on Earth: Nature, v. 570, p. 52–57, https://doi.org/10.1038/s41586-019-1258-4.
- Timmons, J.M., Karlstrom, K.E., Dehler, C.M., Geissman, J.W., and Heizler, M.T., 2001, Proterozoic multistage (ca. 1.1 and 0.8 Ga) extension recorded in the Grand Canyon Supergroup and establishment of northwest- and northtrending tectonic grains in the southwestern United States: Geological Society of America Bulletin, v. 113, p. 163–181, https://doi.org/10.1130/0016-7606(2001)113
 CAGE>2.0.CO;2.
- Whitmeyer, S.J., and Karlstrom, K.E., 2007, Tectonic model for the Proterozoic growth of North America: Geosphere, v. 3, p. 220–259, https://doi.org/10.1130/GES00055.1.
- Yonkee, W.A., Dehler, C.D., Link, P.K., Balgord, E.A., Keeley, J.A., Hayes, D.S., Wells, M.L., Fanning, C.M., and Johnston, S.M., 2014, Tectono-stratigraphic framework of Neoproterozoic to Cambrian strata, west-central U.S.: Protracted rifting, glaciation, and evolution of the North American Cordilleran margin: Earth-Science Reviews, v. 136, p. 59–95, https://doi.org/10.1016/j.earscirev.2014.05.004.

Printed in USA